SHEAR STRENGTH OF HIGH STRENGTH CONCRETE BEAMS REINFORCED BY GFRP AND HTS BARS

Youssef H. Hammad[1], Ibrahim G. Shaaban[2], Ibrahim M. Bazzan[3] and Walid H. Awwad[4]
Civil Engineering Department, Faculty of Engineering, Shoubra, Zagazig University
[1] Professor of Reinforced Concrete Structures, [2] Associate Professor, [3] Assistant Professor and [4] Graduate Student

ABSTRACT

Ten simply supported reinforced concrete beams, with web reinforcement in the form of vertical stirrups, were tested under two symmetrically concentrated loads to investigate the shear strength of High-Strength Concrete (HSC) T-beams reinforced by Glass Fiber Reinforced Plastics (GFRP) and High Tensile Steel (HTS). Nine of the studied beams were made of HSC with mean compressive strength 70 N/mm², five of them were reinforced by HTS bars and the other four specimens were reinforced by GFRP bars as main reinforcement. The control beam was made of normal strength concrete (NSC) with compressive strength 30 N/mm² and reinforced by HTS bars as main reinforcement. All beams were designed according to the provisions of (ACI 318-99). The studied parameters were the amount of web reinforcement (μ_V), the shear span to depth ratio (a/d), and the type of main reinforcement (GFRP or HTS). The actual shear strength of each beam was compared with the predicted strength by different codes of practice for NSC beams reinforced by FRP bars such as (JSCE-97), (CHBDC-Draft-98), and (ACI-440-2001) codes in order to assess the validity of such codes when applied to HSC beams reinforced by GFRP with web reinforcement and to establish an empirical formula for the analysis and design of HSC beams reinforced with GFRP bars. Within the limits of the test results of this research it was concluded that, for beams reinforced by GFRP, the flexural reinforcement ratio (μ) must be increased to about ($1.4\,\mu_b$), as recommended by (ACI 400-2001), to make the design equations of (JSCE-97), (CHBDC, Draft-98), and (ACI 400-2001) applicable for predicting the shear strength of HSC members reinforced by FRP bars, and there was no NA existed after passing the cracking load P_{cr}. Lower stiffness and low modulus of elasticity in GFRP bars relative to HTS resulted in higher crack width; the crack width in beams reinforced by GFRP was six to nine times that of Beams reinforced by HTS. The proposed design formula showed a reasonable accuracy.

Keywords: High-strength concrete, shear reinforcement, shear strength, GFRP, reinforced concrete, T-beams, analysis and design.

INTRODUCTION

It is generally agreed that reinforced concrete beams should have adequate shear reinforcement to prevent sudden and brittle failure after formation of the diagonal crack, and also to keep crack width at an acceptable level [1]. The concrete component V_C is the sum of the resistances to shear due to various shear mechanism. Joint ACI-ASCE-426 [2] lists three separate shear mechanisms; Un-cracked Concrete, which occurs in un-cracked members or un-cracked portion of cracked members; Aggregate Interlock, which occurs between two slip surfaces in the cracked portion of the beam; and Dowel Action at which the longitudinal reinforcement resists part of the shear displacement by dowel forces in the bar [2].

Over the last fifteen years, improvements in material technology and production of ready mixed concrete have resulted in the availability of higher concrete strength grades. The term HSC refers to concrete which has a uni-axial compressive strength greater than that ordinarily obtained in a region. The maximum concrete strength currently being produced varies considerably form region to region in the same country. HSC generally permits more economical construction due to reduced structural member dimensions, this result in a reduction in the dead loads [3].

Fiber reinforced plastics (FRP) reinforcing bars are currently available as a substitute for steel reinforcement in those concrete structures that may be vulnerable to attack by aggressive and corrosive agents. In addition to superior durability, FRP reinforcing bars have much higher strength than conventional steel reinforcing bars, but their moduli are generally lower than that of conventional steel [4]. Because GFRP and HTS bars have different properties, including the modulus of elasticity E, surface characteristics, and bonding characteristics, the shear strength of concrete members reinforced longitudinally by GFRP bars may differ from those reinforced by HTS [5].

Nawy and Neuwerth [6, 7] concluded that, for concrete beams reinforced with GFRP bars, the reinforcing ratio did not affect the moment capacity because the beams failed by crushing of concrete in the compression zone, thus not developing the full capacity of the FRP. In addition, the behavior of the beams with respect to cracking, ultimate load, and deflection could be predicted with the same degree of accuracy as for concrete beams reinforced by steel. Saadatmanesh and Ehsani [8] found that, specimens reinforced with FRP stirrups and longitudinal steel reinforcement failed as a result of yielding in the longitudinal bars. Satoh, et al [9] showed that, the failure load for concrete beams reinforced with FRP can be calculated using elastic theory. Faza and GangaRao [10] reported that HSC must be used instead of NSC for concrete beams reinforced with FRP reinforcing bars in order to take advantage of the high ultimate strength of FRP reinforcing bars. Benmokrane, et al [11, 12] concluded that, at low loads crack pattern and spacing in concrete beams reinforced with FRP reinforcing bars were similar to those in conventionally reinforced beams. In addition, at service load, there were more and wider cracks with greater penetration in concrete beams reinforced with FRP reinforcing bars than conventionally reinforced concrete therefore, since corrosion is not an issue with FRP reinforcing bars, crack width should be redefined on a basis other than corrosion. Zia et al [13] found that no shear failure was developed for concrete beams reinforced with FRP bars but the beams failed due to tensile rupture of the longitudinal FRP bars.

Objective and Aims of the Present Study

The present investigation is a part of a larger research performed to study the shear behavior of HSC beams reinforced by GFRP and HTS with different web reinforcement and shear span to depth ratio [14].

Because there are fundamental differences in the properties of HTS and GFRP bars and due to the empirical nature of shear design methods, investigations are required to determine if these methods are applicable when GFRP reinforcement are used. The main objective was to evaluate the applicability of current design codes for shear such as (JSCE-97) [15], (CHBDC-Draft-98) [16], and (ACI-440-2001) [17] to HSC beams with web reinforcement in the form of vertical stirrups and longitudinally reinforced by HTS and GFRP bars. In addition, an empirical formula was developed for the analysis and design of HSC beams reinforced with GFRP as main reinforcement.

TEST PROGRAM AND EXPERIMENTAL WORK

Test Specimens

The test program consisted of ten simply supported reinforced concrete beams with web reinforcement in the form of vertical stirrups. All the studied beams were T-shaped in cross section as shown in Figure 1. Table 1 shows a description of the test beams along with the studied parameters and the actual cube compressive strength for the different specimens. The main reinforcement ratio in all the test beams was kept constant of ($\mu = 0.85\mu_b$). Two different mixes were used to develop normal and high strength concrete at 28 days of target strength 30 and 70 N/mm², respectively. Table 2 shows the mix designs for the two concrete strengths. The used GFRP bars were fabricated from vinyl ester with an outer coat to seal the bar. The bar is produced using drown continuous “C “glass rovings and has a longitudinal irregular surface. A single strand spiral wrap around the outside diameter produces a spiral indentation in the bar. The properties of the GFRP bars were given by the producing factory [18]. The average results of the used GFRP and HTS are shown in Table 3.

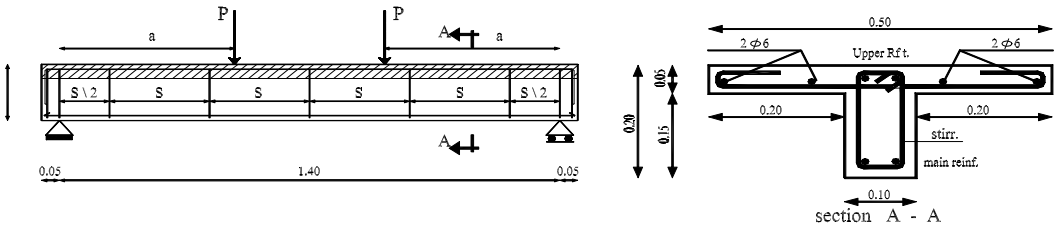

Fig. 1 Details of test beams.

Table 1 Description of Test Beams and Studied Parameters

Beam	f_{cu}	$\mu_s = A_s/bd$	Reinforcement	$\mu_v = A_v/bS$	No. Of stirrups	a/d
B1	30	2.83 %(H.T.S)	4 Φ 12	0.202	Ø6 @ 280 mm	2.5
B2	68.8	3.93 %(H.T.S)	2 Φ 16 + 2 Φ 12	0.202	Ø6 @ 280 mm	1.5
B3	68.8	3.93 %(H.T.S)	2 Φ 16 + 2 Φ 12	0.202	Ø6 @ 280 mm	2.5
B4	67.5	3.93 %(H.T.S)	2 Φ 16 + 2 Φ 12	0.202	Ø6 @ 280 mm	3.5
B5	69.2	3.93 %(H.T.S)	2 Φ 16 + 2 Φ 12	0.324	Ø6 @ 175 mm	2.5
B6	67.5	3.93 %(H.T.S)	2 Φ 16 + 2 Φ 12	0.503	Ø8 @ 200 mm	2.5
B7	71.2	0.53%(GFRP)	3 ¢ 6	0.202	Ø6 @ 280 mm	1.5
B8	71.4	0.53%(GFRP)	3 ¢ 6	0.202	Ø6 @ 280 mm	2.5
B9	67.7	0.53%(GFRP)	3 ¢ 6	0.324	Ø6 @ 175 mm	2.5
B10	71.5	0.53%(GFRP)	3 ¢ 6	0.202	Ø6 @ 280 mm	3.5

f_{cu} = Average cube compressive strength of concrete, N/mm².
μ_s = Longitudinal steel ratio,
μ_v = Web steel ratio,
Φ = Bar diameter, HTS,
Ø = Bar diameter, ordinary mild steel,
a/d = shear span to depth ratio,
¢ = Bar diameter, GFRP

Table 2 Concrete Mix-Design

Mix No.	Cement kN	Sand kN	Crushed Basalt kN	Silica fume kN	Water kN	Super-plasticizers kN
1	3.50	6.40	11.80	---	1.80	---
2	5.50	5.50	11.25	0.80	1.60	0.23

Table 3 Results of the test steel and GFRP Specimens

Reinforcement	Yield Strength N/mm²	Ult. Strength N/mm²	Young Modulus kN/mm²	Elongation
Mild Steel	283.0	396.0	200.0	26%
HTS	436.0	602.8	200.0	17%
GFRP	----	580.0	40.0	3.5%

Test Procedure

Each beam was tested as simply supported beam under two vertical concentrated loads using two vertical hydraulic jacks which were similar in their acting position and value. The vertical loads were applied in increments (20 kN for beams reinforced by HTS and 5 kN for beams reinforced by GFRP). After each increment, the strains in the main steel and stirrups were measured using electrical strain gauges of length 5 mm, resistance 120.4 ± 0.4 ohm, and a gauge factor of 2.11. Detection of cracks and marking them for each incremental load were made when the load reached its steady state.

ANALYSIS AND DISCUSSION OF THE TEST RESULTS

Deflection Profiles

The deflection profile of the test beams plotted at three stages just before cracking load (P_{cr}), at working load (P_w) (approximately 67% of failure load), and at failure load (P_f). In general, for all the test beams, the deflection profile was approximately symmetric with respect to the vertical axis passing through the mid span of the beams. The symmetric condition violated in a small order, with increasing the applied load. The effects of the studied parameters such as shear span to depth ratio, the amount of web reinforcement and the type of main reinforcement (GFRP and HTS) on the deflection profile of the studied beams were illustrated in Figure 4.

It can be seen from Figures 4.-b, c, d, e, and f, (Beams from B2 through B6 reinforced by HTS), that increasing the load from P_{cr}, to P_w, and to P_f, lead to a gradual increasing in the deflection values (see Table 5) with gentle curvature of the deflection profile. In addition, it can be seen from Figures 4.5-g, h, i, and j, (Beams from B7 through B10 reinforced by GFRP), that increasing the load from P_{cr} to P_w and to P_f lead to a very large increasing in the deflection values (see Table 5) with steeper curvature of the deflection profile.

It can be seen from Figures 4-g, h, and j, that increasing a/d from 1.5 for Beam B7 to 3.5 for Beam B10 resulted in increasing the deflection by approximately 50% as the load increased from P_{cr} to P_w, and by approximately 41% as the load increased from P_{cr} to P_f. It was also observed from Figures 4.5-a, and 4.5-h, that the deflection of the control NSC Beam B1 increased by approximately 12% as the load increased from P_{cr} to P_w, and by approximately 96% as the load increased from P_{cr} to P_f, compared with those of Beam B8.

It can be seen from Figures 4-h, and 4-i, that increasing μ_V from 0.202 for Beam B8 to 0.324 for Beam B9 lead to increasing the deflection by approximately 19% as the load increased from P_{cr} to P_w, while increasing the load from P_{cr} to P_f lead to further increasing in the deflection by approximately 15%.

It can be seen from Figures 4-b through 4-i, that increasing the load from P_{cr} to P_w lead to increasing the deflection for Beams B7, B8, B9, and B10 (reinforced by GFRP) more than that for Beams B2, B3, B5, and B4 (reinforced by HTS) by approximately 116%, 123%, 115%, and 164% respectively. In addition, increasing the load from P_{cr} to P_f leaded to further increasing in the deflection by approximately 158%, 169%, 168%, and 209% respectively.

Table 5 Deflection Values of the test beams at P_{cr}, P_w and P_f

Beam	B1	B2	B3	B4	B5	B6	B7	B8	B9	B10
P_{cr}	0.39	0.37	0.47	0.55	0.66	0.74	0.30	0.35	0.444	0.50
P_w	3.50	3.10	3.54	3.90	4.45	5.15	6.20	7.30	8.60	9.35
P_f	8.18	5.49	6.14	6.60	7.21	8.01	13.52	15.58	18.02	19.19

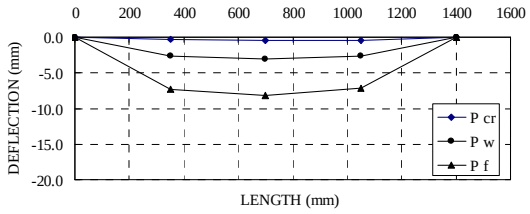

(a)Beam B1 (a/d=2.5, μ_V =0.202 and HTS)

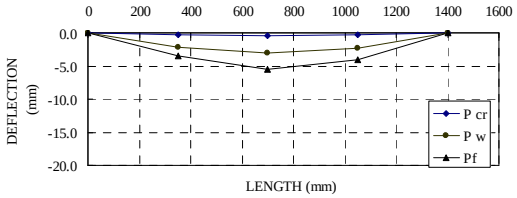

(b) Beam B2 (a/d=1.5, μ_V =0.202 and HTS)

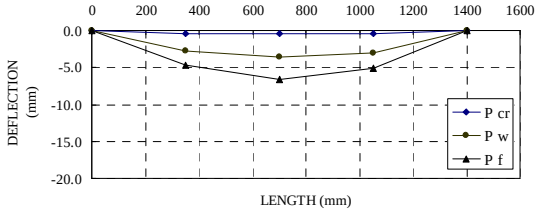

(c) Beam B3 (a/d=2.5, μ_V =0.202 and HTS)

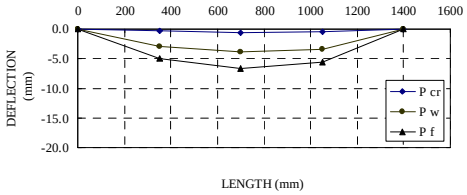

(d) Beam B4 (a/d=3.5, μ_V =0.202 and HTS)

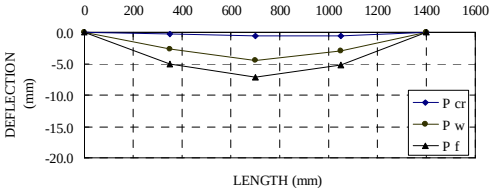

(e) Beam B5 (a/d=2.5, μ_V =0.324 and HTS)

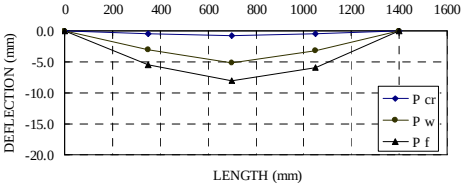

(f) Beam B6 (a/d=2.5, μ_V =0.503 and HTS)

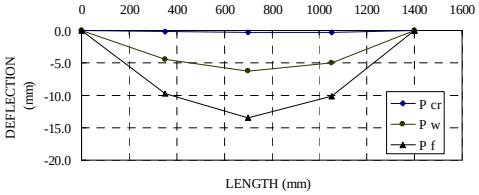

(g) Beam B7 (a/d=1.5, μ_V =0.202 and GFRP)

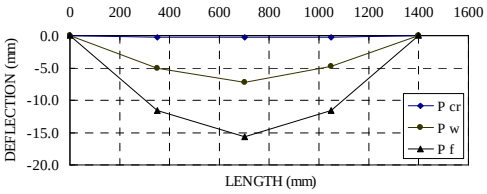

(h) Beam B8 (a/d=2.5, μ_V =0.202 and GFRP)

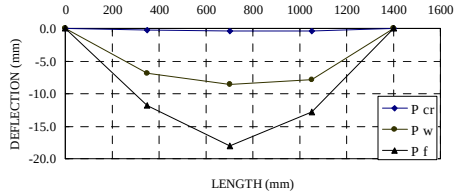

(i) Beam B9 (a/d=2.5, μ_V =0.324 and GFRP)

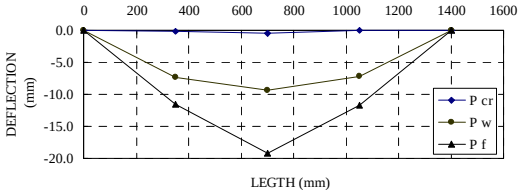

(j) Beam B10 (a/d=3.5, μ_V =0.202 and GFRP)

Figure 4 Deflection Profiles of the Test Beams

Concrete Strain-Profiles

Figure 5 shows the mid span concrete strain-profile of the test beams at P_{cr}, P_w and P_f. It can be seen from Figures 5-a through 5-f, that, for Beams from B1 through B6 (reinforced by HTS), the profile curves at P_{cr}, P_w and P_f intersected together to give the position of the Neutral Axis (NA) very close to the vertical axis at a distant, measured from the bottom of the beam web, changing according to the effect of the studied parameters (a/d, and μ_V). In addition, it can be seen from Figures 5-g through 5-j, that, for Beams B7 through B10 (reinforced by GFRP), the profile curves at P_{cr}, P_w and P_f did not intersect together or with the vertical axis to give the position of the NA.

It can be seen from Figures 5-b through 5-d that, increasing a/d from 1.5 for Beam B2 to 2.5 for Beam B3 lead to increasing the distant of the NA position, measured from the bottom of the beam web, from approximately 132 mm to approximately 148 mm (i.e. the compression zone reduced by approximately 12%). Further increasing in the distant of the NA position to approximately 180 mm took place by increasing a/d to 3.5 for Beam B4 (i.e. the compression zone reduced by approximately 36%). Moreover, it can be seen from Figures 5-a and 5-c, that the distant of the NA position of Beams B1 and B3 were 160 mm and 148 mm respectively. The compression zone of Beam B3 was more than that of Beam B1 by approximately 8%.

It can be seen from Figures 5-c, 5-e, and 5-f, that increasing μ_V from 0.202 for Beam B3 to 0.324 for Beam B5 lead to increasing the distant of the NA position from approximately 148 mm to approximately 188 mm (i.e. the compression zone reduced by approximately 27%). Further increasing in the distant of the NA position to approximately 193mm took place by increasing μ_V to 0.503 for Beam B6 (i.e. the compression zone reduced by approximately 30%).

Figures 5-g through 5-j (beams B7 through B10 reinforced by GFRP) show that the profile curve at P_{cr} was very close to the vertical axis and intersect with it, while the other two profile curves at P_w and P_f were fare from the vertical axis and the profile curve at P_{cr} by a distant increased by increasing a/d from 1.5 for Beam B7 to 3.5 For beam B10, and decreased by increasing μ_V from 0.202 for Beam B8 to 0.324 For Beam B9. There was no NA existed after passing the cracking load P_{cr}.

It can be seen, from Figure 5, that the effect of shear span to depth ratio (a/d) is more significant than that of increasing the web reinforcement (μ_V), while changing the type of main reinforcement from HTS to GFRP resulted in reducing the compression zone which performed at the stage of the P_{cr}. Exactly after the stage of P_{cr} the full cross-section exhibited complete tension stresses without any compression zone. There was no NA for beams reinforced by GFRP bars; this may be attributed to the low reinforcing ratio of GFRP bars $\mu = 0.58\mu_b$.

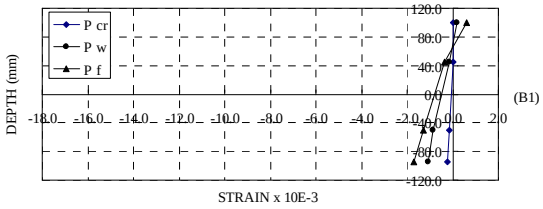

(a) Beam B1 (a/d=2.5, μ_V =0.202 and HTS)

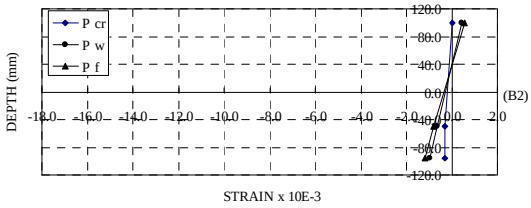

(b) Beam B2 (a/d=1.5, μ_V =0.202 and HTS)

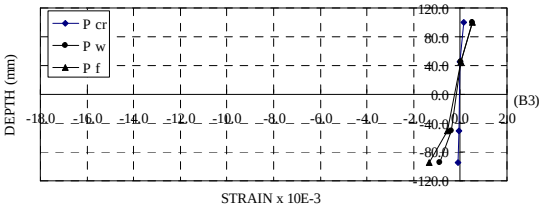

(c) Beam B3 (a/d=2.5, μ_V =0.202 and HTS)

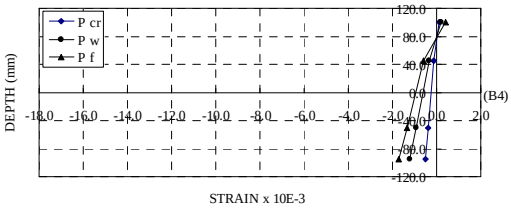

(d) Beam B4 (a/d=3.5, μ_V =0.202 and GFRP)

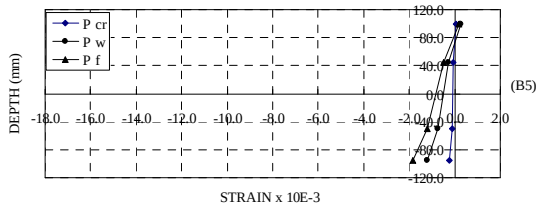

(e) Beam B5 (a/d=2.5, μ_V =0.324 and HTS)

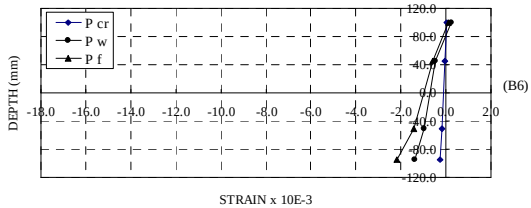

(f) Beam B6 (a/d=2.5, μ_V =0.503 and HTS)

Figure 5 Concrete Strain-Profiles of the Test Beams

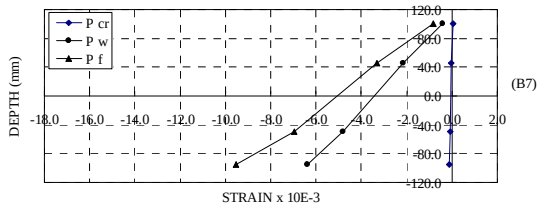

(g) Beam B7 (a/d=1.5, μ_V =0.202 and GFRP)

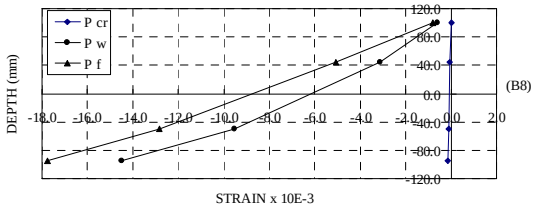

(h) Beam B8 (a/d=2.5, μ_V =0.202 and GFRP)

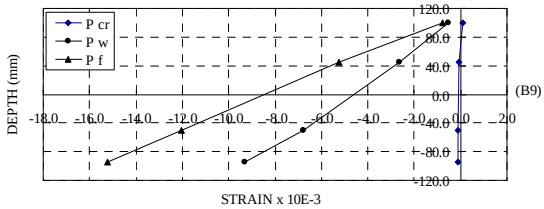

(i) Beam B9 (a/d=2.5, μ_V =0.324 and GFRP)

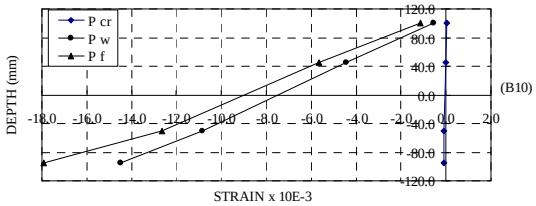

(j) Beam B10 (a/d=3.5, μ_V =0.202 and GFRP)

Figure 5 Concrete Strain-Profiles of the Test Beams (Continued)

Crack Width

The effects of the studied parameters such as shear span to depth ratio (a/d), the amount of web reinforcement(μ_V), and the type of main reinforcement (HTS and GFRP) on the relation between the ultimate measured load capacity and the corresponding crack width were illustrated in Figures from 6 through 8. Crack width of the test beams was measured using mechanical gauges of 150 mm gauge lengths and 0.001 mm accuracy.

It can be seen from Figure 6 that increasing a/d from 1.5 for Beam B7 to 2.5 for Beam B8 lead to increasing the maximum crack width by approximately 19%. Further increasing the maximum crack width by approximately 66, took place by increasing a/d to 3.5 for Beam B10. It was also observed from Figure 6, that the control NSC Beam B1 had a smaller crack width by approximately 79%, compared with that of Beam B8.

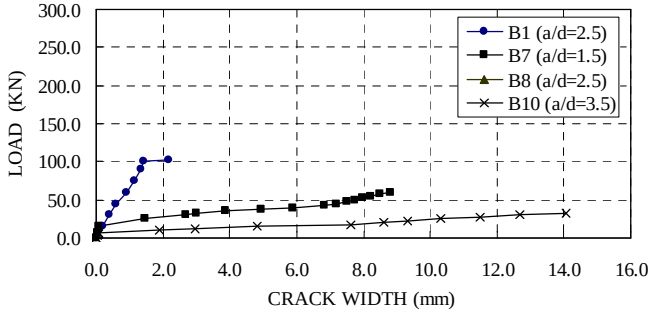

Beams Reinforced by GFRP bars and μ_V =0.202

Figure 6 Effect of Span/Depth (a/d) on the Load-Crack Width Relationship

It can be seen from Figure 7, that increasing μ_V from 0.202 for Beam B8 to 0.324 for Beam B9 lead to increasing the maximum crack width by approximately 52%.

It can be seen from Figures 8-a, b, c, and d, that the maximum crack width of Beams B7, B8, B10, and B9 was more than that of Beams B2, B3, B4, and B5 by approximately 686%, 729%, 597%, and 769% respectively.

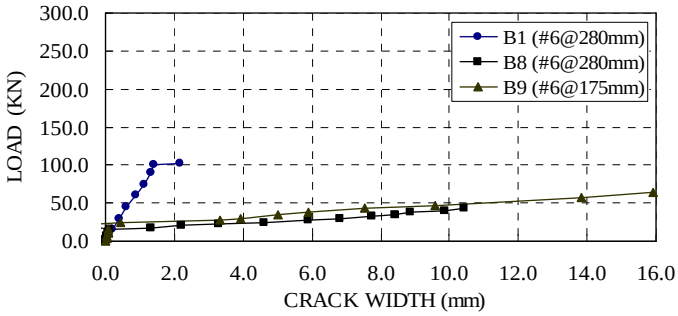

Beams Reinforced by GFRP bars and a/d=2.5

Figure 7 Effect of Web Reinforcement Ratio (μ_V) on the Load-Crack Width Relationship

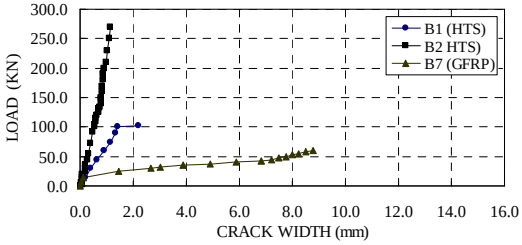

(a) Beams with a/d=1.5 and μ_V =0.202

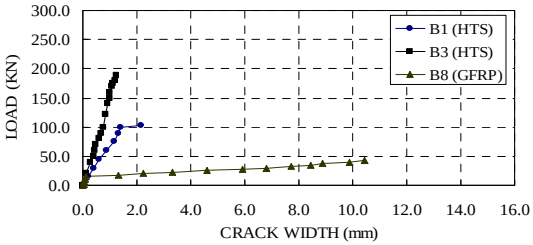

(b) Beams with a/d=2.5 and μ_V =0.202

Figure 8 Effect of Type of Main Reinforcement on the Load-Crack Width Relationship

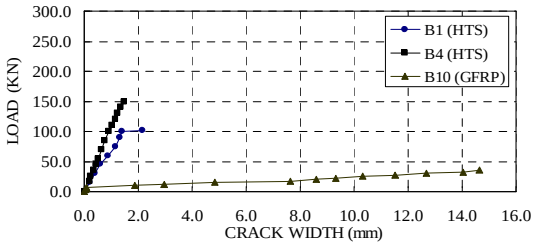

(c) Beams with a/d=3.5 and μ_V =0.202

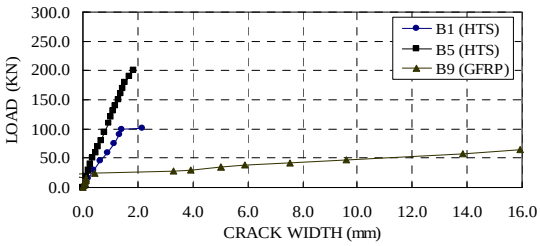

(d) Beams with a/d=2.5 and μ_V =0.324

Figure 8 Effect of Type of Main Reinforcement on the Load-Crack Width Relationship (Continued)

It can be seen from Figures 6 and 7 that the effect of shear span to depth ratio (a/d) is more significant than that of increasing the web reinforcement (μ_V). Lower stiffness and low modulus of elasticity in GFRP bars relative to HTS resulted in higher crack widths. It was observed from Figure 8 that the crack width in Beams B7, B8, B9, and B10 (reinforced by GFRP) is six to nine times that in Beams B2, B3, B4, and B5 (reinforced by HTS). In addition, there were more and wider cracks with greater penetration. Since corrosion is not an issue with GFRP reinforcing bars, it follows that the acceptable admissible crack width should be redefined on a basis other than corrosion.

THEORETICAL PREDICTION OF EXPERIMENTAL RESULTES

Many major concrete codes from around the world are based on research conducted on structural members made of NSC. Recently, some concrete codes have included provisions for the design of HSC members. Extrapolations of design rules meant for NSC for

use with HSC may not be always, appropriate. If failure was brittle or non-ductile failure, as with shear failure, extrapolating existing NSC design rules for HSC may result in less or non-conservative design criteria; therefore it is very important to estimate empirical formulae for the analysis and design of HSC beams reinforced with GFRP bars based on experimental work [19].

Proposed Equation

The ultimate shear capacity of HSC beams reinforced by GFRP can be calculated from applying Equation 1 which was modified from The Equation made by (CHBDC, Draft-98) [16].

$$V_{u(prop)} = 0.032\phi_c \left(f_{cu} \mu E_f \frac{V_u}{M_u} d \right)^{1/5} + \frac{A_v f_{yv}}{b_w S} \quad (1)$$

Comparison of Test Results with Codes

The results of the test beams were predicted by relevant codes of practice such as Japanese Society of Civil Engineering Code (JSCE-97) [15], Canadian Highway Bridge Design Code (CHBDC, Draft-98) [16], American Code (ACI 440-2001) [17], and the proposed equation, to assess the validity of such codes when applied to HSC beams reinforced by GFRP bars as main reinforcement and with vertical web reinforcement. The prediction of test results by the above mentioned codes and the proposed equation is listed in Table 6.

Table 6 shows that for beams reinforced by HTS, the shear strength predicted by (ACI 400-2001) [17] and the proposed equation were conservative to different degrees. On the other hand, shear strength predicted using (CHBDC, Draft-98) [16] was not conservative for NSC Beam B1 and HSC Beam B4 (with increasing a/d to 3.5). In addition, the shear strength predicted using (JSCE-97) [15] was unsafe for all the test beams. For beams reinforced by GFRP bars, the situation was different. The shear strength predicted by (JSCE-97) [15], (CHBDC, Draft-98) [16], and (ACI 400-2001) [17] were not conservative at all. It can be argued that the flexural reinforcement ratio (μ) must be increased to approximately ($1.4\mu_b$), as recommended by (ACI 400-2001) [17], to make the design equations of (JSCE-97) [15], (CHBDC, Draft-98) [16], and (ACI 400-2001) [17] applicable for predicting the shear strength of HSC members reinforced by FRP bars. Unlike the studied codes, the proposed equation was conservative and more accurate for predicting the shear strength for all the studied beams, reinforced by GFRP bars, to different degrees.

Table 6 Prediction of Shear Strength by Different Codes of Practices and the Proposed Equation

Beam No.	Reinf.	μ_v	a/d	$\frac{V_{Test}}{V_{JSCE}}$	$\frac{V_{Test}}{V_{CHBDC}}$	$\frac{V_{Test}}{V_{ACI}}$	$\frac{V_{Test}}{Vproposed}$
B1	HTS	0.202	2.5	0.275	0.764	2.269	2.929
B2	HTS	0.202	1.5	0.500	1.246	4.607	6.540
B3	HTS	0.202	2.5	0.348	1.014	3.208	4.837
B4	HTS	0.202	3.5	0.278	0.896	2.560	4.010
B5	HTS	0.324	2.5	0.370	1.025	2.922	4.106
B6	HTS	0.503	2.5	0.400	1.031	2.605	3.418
B7	GFRP	0.202	1.5	0.205	0.470	0.956	1.694
B8	GFRP	0.202	2.5	0.145	0.385	0.677	1.262
B9	GFRP	0.324	2.5	0.222	0.537	0.887	1.470
B10	GFRP	0.202	3.5	0.120	0.348	0.558	1.072

Table 6 shows that, for Beams reinforced by HTS, the proposed equation was less conservative with increasing a/d. It was observed that increasing a/d from 1.5 for Beam B2 to 2.5 for Beam B3 lead to a reduction of the over estimated value of the shear strength by approximately 26%, while increasing a/d to 3.5 for Beam B4 resulted in further reduction of the over estimated value of the shear strength by approximately 39%. In addition, the proposed equation was less conservative with increasing μ_v. Table 6 shows that increasing μ_v from 0.202 for Beam B3 to 0.324 for Beam B5 lead to a reduction of the over estimated value of the shear strength by approximately 15%, while increasing μ_v to 0.503 for Beam B6 resulted in further reduction of the over estimated value of the shear strength by approximately 29%.

Table 6 shows that, for Beams reinforced by GFRP, the proposed equation was less conservative with increasing a/d. It was observed that increasing a/d from 1.5 for Beam B7 to 2.5 for Beam B8 lead to a reduction of the over estimated value of the shear strength by approximately 26%, while increasing a/d to 3.5 for Beam B10 resulted in further reduction of the over estimated value of the shear strength by approximately 37%. In addition, the proposed equation was more conservative with increasing μ_v. Table 6 shows that increasing μ_v from 0.202 for Beam B8 to 0.324 for Beam B9 lead to increasing the over estimated value of the shear strength by approximately 16%.

Table 6 shows that the (CHBDC, Draft-98) [16] was less conservative with increasing a/d. It was observed that increasing a/d from 1.5 for Beam B2 to 2.5 for Beam B3 lead to a reduction of the over estimated value of the shear strength by approximately 19%, while increasing a/d to 3.5 for Beam B4 lead to under estimation of the results. In addition, the (CHBDC, Draft-98) [16], was more conservative with increasing μ_v. Table 6 shows that increasing μ_v from 0.202 for Beam B3 to 0.324 for Beam B5 lead to increasing the over estimated value of the shear strength by approximately 11%, while increasing μ_v to 0.503 for Beam B6 resulted in further increasing in the over estimated of the shear strength by approximately 17%.

It can be seen from Table 6 that the American Code (ACI-400-2001) [17] was less conservative with increasing a/d. It was observed that the ACI-400-2001 was less conservative by approximately 30% with increasing a/d from 1.5 for Beam B2 to 2.5 for Beam B3, while it was less conservative by approximately 44% with increasing a/d to 3.5 for Beam B4. In addition, the American Code (ACI-400-2001) [17] was less conservative with increasing μ_v. It can be seen from Table 6 that the ACI-400-2001 was less conservative by approximately 9% with increasing μ_v from 0.202 for Beam B3 to 0.324 for Beam B5, while it was less conservative by approximately 19% with increasing μ_v to 0.503 for Beam B6.

It can be seen from Table 6 that the effect of the shear span to depth ratio (a/d) is more significant than that of increasing the web reinforcement (μ_V).

CONCLUSIONS

The aim of this research was to evaluate the applicability of current design codes for shear such as (JSCE-97) [15], (CHBDC-Draft-98) [16], and (ACI-440-2001) [17] to HSC T-beams with web reinforcement in the form of vertical stirrups and longitudinally reinforced by HTS and GFRP bars. Ten simply supported reinforced concrete beams were tested experimentally under two symmetrically concentrated loads. Nine of the studied beams were made of HSC with mean compressive strength 70 N/mm², five of them were reinforced by HTS bars and the other four specimens were reinforced by GFRP bars as main reinforcement. The control beam was made of NSC with compressive strength 30 N/mm² and reinforced by HTS bars as main reinforcement. The web reinforcement for all the test beams was in the form of vertical stirrups. All beams were designed according to the previsions of ACI 318-99 [20]. The studied parameters were the amount of web reinforcement (μ_V), shear spans to depth ratio (a/d) and type of main reinforcement (GFRP and HTS). Actual shear strength of each beam was compared with the predicted strength using different codes of practice such as (JSCE-97) [15], (CHBDC-Draft-98) [16], and (ACI-440-2001) [17] and the proposed equation in order to establish empirical formula for the analyses and design of HSC beams

reinforced with GFRP bars. Based on the experimental results in this paper, the following conclusions, for HSC beams reinforced with GFRP bars, can be summarized as follows:

1. For beams reinforced by HTS, increasing shear span to depth ratio (a/d) from 1.5 to 3.5 lead to increasing the distant of the NA position, measured from the bottom of the beam web, from approximately 132 mm to approximately 180 mm (i.e. the compression zone reduced by approximately 36%), and increasing the cracks width by approximately 31%.In addition increasing μ_V from 0.202 to 0.503 resulted in decreasing cracks spacing while the number of cracks and crack width increased, increasing the distant of the NA position, from approximately 148 mm to approximately 193 mm (i.e. the compression zone reduced by approximately 30%), and increasing the cracks width by approximately 77%.
2. For beams reinforced by GFRP, increasing a/d from 1.5 to 3.5 resulted in increasing the maximum deflection by approximately 41% as the load increased from P_{cr} to P_f, and increasing the cracks width by approximately 66%. In addition, increasing the amount of web reinforcement μ_V from 0.202 to 0.324 resulted in increasing the maximum deflection by approximately 15% as the load increased from P_{cr} to P_f, and increasing the cracks width by approximately 53%. There was no NA existed after passing the cracking load P_{cr}.
3. Changing the type of main reinforcement from HTS to GFRP lead to increasing the maximum deflection by approximately 176% as the load increased from P_{cr} to P_f, and increasing the cracks width by approximately 750%.
4. The cracks width in Beams reinforced by GFRP was found to be six to nine times that of Beams reinforced by HTS, and there were more and wider cracks with greater penetration, hence, since corrosion is not an issue with GFRP reinforcing bars, it follows that the acceptable admissible crack width should be redefined on a basis other than corrosion.
5. For HSC beams reinforced by HTS, the predicted shear strength using (ACI 400-2001) was conservative to different degrees. In addition, the predicted shear strength using (CHBDC, Draft-98) was not conservative for NSC beam reinforced by HTS and HSC beams with increasing a/d. Moreover, the predicted shear strength using (JSCE-97) was not conservative at all.
6. For HSC beams reinforced by GFRP bars, the shear strength predicted using (JSCE-97), (CHBDC, Draft-98), and (ACI 400-2001) was not conservative at all.
7. The proposed equation was conservative and more accurate than the relevant codes of practice for NSC beams reinforced by FRP bars. The proposed equation was over estimating the shear strength values for the test beams reinforced by HTS. The prediction was sensitive to the effect of shear span to depth ratio (a/d), and the web reinforcement ratio (μ_V).

ACKNOWLEDGEMENT

The authors wish to express their sincerest thanks and gratitude to Prof. Dr. Omar El-Nawawy, Professor of Reinforced Concrete Structure, and Assist. Prof. Dr. Ayman Hussain Hosny Khalil, Assistant Professor, Faculty of Engineering, Ain Shams University, for providing the authors with the GFRP rods used in this investigation. In addition, the authors are also grateful to all members of the staff and technicians, of the Reinforced Concrete Testing Laboratory, Faculty of Engineering, Cairo University, for their great help during the experimental phase of this investigation.

REFERENCES

1. Ozcebe Guney, Ersoy Ugur, and Tankut Tugrul “Evaluation of Minimum Shear Reinforcement Requirements for High Strength Concrete “ACI Structural Journal / May-June 1999.

2. ACI-ASCE Committee 426, “The Shear Strength of Reinforced Concrete Members, “Journal of Structural Division, ASCE, V. 99, No. ST6, June1973, pp.1091-1187.
3. “State-of-the-Art Report on High Strength Concrete “Reported by Committee 363, ACI 363R-97.
4. Razaqpur A.G., Svecova Dagmar, and Cheung M.S., “Rational Method for Calculating Deflection of Fiber Reinforced Polymer Reinforced Beams,” ACI Structural Journal, V.97, No. 1, January-February, pp.175-184, 2000.
5. Tureyen A. Koray and Frosch Robert J., “Shear Tests of FRP-Reinforced Concrete Beams without Stirrups,” ACI Structural Journal, July-August, pp.427-434, 2002.
6. Nawy, E.G., and Neuwerth, G. E., “Behavior of Fiber Glass Reinforced Concrete Beams," Journal of Structural Division, ASCE, September 1971, pp. 2203-2215.
7. Nawy, E.G., and Neuwerth, G. E., “Fiber Glass Reinforced Concrete Slabs and Beams," Journal of Structural Division, ASCE, February 1977, pp. 421-440.
8. Saadatmanesh, H., and Ehsani, M. R., "Fiber Composite Bar for Reinforced Concrete Construction," Journal of Composite Materials, V. 25, February 1991, pp. 188-203.
9. Satoh, K.; Kodama, K.; and Ohki, H., " A Study on the Bending Behavior of Repaired Reinforced Concrete Beams Using Fiber Reinforced Plastic (FRP) and Polymer Mortar," Evaluation and Rehabilitation of Concrete Structures and Innovations in Design, Proceedings ACI International Conference, Hong Kong, 1991, pp. 1017-1031.
10. Faza, S. S., and GangaRao, H. V. S., " Bending and Behavior of Concrete Beams Reinforced with Fiber Reinforced Plastic Rebars," WVDOH-RP-83 Phase 1 Report, West Virginia University, Morgantown, 1992, pp. 128-173.
11. Benmokrane, O. Chaallal, and R. Masmoudi “Flexural Response of Concrete Beams Reinforced with FRP Reinforcing Bars “ACI Structural Journal / January-February 1996.
12. Radhouane Masmoudi, Michele Theriault and Brahim Benmokrane “ Flexural Behavior of Concrete Beams Reinforced with Plastic Reinforcing Rods “ACI Structural Journal / November-December 1998.
13. Zia, P.; Ahmad, S.; Garg, R.; and Hanes, K., " Flexural and Shear Behavior of Concrete Beams Reinforced with #D Continuous Carbon Fiber Fabric," Concrete International, V. 14, No. 12, December 1992, pp. 48-52.
14. Awwad Walid H. "Shear Behavior of Reinforced High Strength Concrete Beams" Faculty of Engineering, Shoubra, Zagazig University
15. Japan Society of Civil Engineers, “Recommendations for Design and Construction of Concrete Structures Using Continuous Fiber Reinforcing Materials, “JSCE, No.30, Japan, December 1997.
16. Canadian Highway Bridge Design Code, CHBDC, (Draft), Canadian Standards Association, Rexdale, Ontario, Canada, 1998.
17. ACI Committee 440, “Guide for the Design and Construction of Concrete reinforced FRP Bars, “American Concrete Institute, Detroit, May 2001.
18. Khalil Ayman Hussein Hosny “Behavior of Concrete Slabs Reinforced With Fiber Glass Rebars “Ain Shams University, M. SC., 1994.
19. Pendyala Raghu S. and Mendis Prian “Experimental study on Shear Strength of High-strength Concrete Beams “ACI Structural Journal / July-August 2000.
20. ACI Committee 318, “Building Code Requirements for Structural Concrete (ACI 318-99) and Commentary (ACI 318R-99),” American Concrete Institute, Detroit, 369 pp., 1999.